Hindawi
Journal of Sensors
Volume 2019, Article ID 7608512, 11 pages
https://doi.org/10.1155/2019/7608512

Research Article

The Registration of a Biomaser-Like Effect in an Enzyme System with an RTM Sensor

Yu. D. Ivanov[1,2] **K. A. Malsagova**[1] **S. G. Vesnin**[3] **V. Yu. Tatur**[4] **N. D. Ivanova**[5] **and V. S. Ziborov**[1,2]

[1] *Institute of Biomedical Chemistry (IBMC), Pogodinskaya Street, 10, build. 8, 119121, Moscow, Russia*
[2] *Joint Institute for High Temperatures of Russian Academy of Sciences, Moscow, Russia*
[3] *RES Ltd, Moscow, Russia*
[4] *Foundation of Perspective Technologies and Novations, Moscow, Russia*
[5] *Skryabin Moscow State Academy of Veterinary Medicine and Biotechnology, Moscow, Russia*

Correspondence should be addressed to Yu. D. Ivanov; yurii.ivanov.nata@gmail.com

Received 27 March 2019; Revised 11 June 2019; Accepted 9 July 2019; Published 21 August 2019

Academic Editor: Carlos Michel

The concentration dependence of a microwave frequency radiation from a solution of a functioning enzyme system (ES) (with the example of cytochrome P450 BM3 (CYP102A1) system during lauric acid (LA) hydroxylation) has been studied with a radiothermometric sensor. Registration of the radiation from the enzyme solution has been performed in the frequency range from 3.4 to 4.2 GHz at the enzyme concentrations from 10^{-10}M to 10^{-6}M. It has been demonstrated that the catalysis of LA hydroxylation in a reconstituted CYP102A1 system is accompanied by a generation of microwave radiation over the entire range of concentrations studied. It has been found that a transition from a multipulse mode (at nanomolar enzyme concentrations from 10^{-10}M to 10^{-8}M) to a single-pulse mode (at micromolar enzyme concentrations from 10^{-7}M to 10^{-6}M) is observed. This effect is discussed on the basis of assumptions considering possible realization of biomaser-like radiation in the enzyme system. The discovered concentration-based effect of the transition of an unsynchronized pulsed radiation into a synchronized one in ES can further be used in the development of novel methods of noninvasive diagnostics of diseases, in mathematical modeling of the functioning of living systems, and in the development of next-generation quantum computers.

1. Introduction

Functioning of enzyme systems (ES) can be considered as a cyclic transition of the system from a nonexcited state to an excited nonequilibrium one and then back to the equilibrium. During the process of catalysis, a visible-range radiation can be observed for a number of enzyme systems, e.g., for the oxidative enzymes that catalyze the reaction followed by bioluminescence, i.e., luciferase [1]. Radiation from enzyme systems can be observed in other spectral ranges as well. In this way, previously it was demonstrated that the functioning of the CYP102A1 enzyme system in a narrow concentration range (from 10^{-9}M to 10^{-8}M) is accompanied by a microwave radiation in the form of pulse trains at 3.4 to 4.2 GHz frequency [2]. In [2], a radiothermometry method was employed. This method is becoming more common for monitoring of functional state of both cellular systems and the whole organism [3, 4]. Radiothermometer (abbreviated, radiometer) measures the object's brightness temperature T_{br}. The brightness temperature (radio temperature) is the temperature value that is numerically equal to the thermodynamic temperature of an ideal black body. In the process of catalytic reaction, a nonequilibrium state of the medium can occur; this state is characterized by an increase in the brightness temperature, what can be accompanied by a radiation in a certain frequency range connected with the increase in the brightness temperature. Thus, the use of a radiometer operating in a microwave range allows one to measure the kinetics of biochemical processes by monitoring changes in the brightness temperature. This approach is very convenient, as it is label-free, does not require expensive equipment, and provides new information about

quantum phenomena in biological systems. Such processes of increase in brightness temperature accompanied by radiation in various spectral ranges, often manifest themselves not only in natural biological systems, but are also observed in gas-discharge devices (including domestic ones), during nonequilibrium processes in shock waves, upon flowing of liquid media through injectors, etc.

The CYP102A1 system was selected to be used in the study in [2] owing to the fact that bacterial enzyme CYP102A1, which pertains to the super family of heme-containing cytochromes P450, plays a crucial role in *Bacillus megaterium* enzymatic pathways [5]. This protein represents a self-sufficient enzyme requiring no any extra partner proteins for the implementation of a catalytic cycle. The enzyme is structured so that its reductase and heme domains are combined in a single polypeptide chain [6]. This stimulates the interest in studying this enzyme as a convenient simplified model of cytochrome P450-containing monooxygenase systems, contributing to oxidation of endogenous and exogenous substrates in an organism [7]. CYP102A1 catalyzes hydroxylation (mainly, (ω-1), (ω-2), and (ω-3)–hydroxylation) of saturated and unsaturated fatty acids with various chain lengths [8]. It was also demonstrated that full-length CYP102A1 can exist in both monomeric and oligomeric states, primarily in the form of dimers (>50%) [9]. Besides, dimeric form exhibits higher activity in comparison with the monomeric one, with k_{cat} of $50s^{-1}$ and $10s^{-1}$ for the dimers and monomers, respectively [10].

The objective of our study is to measure the dependence of a radiation from the CYP102A1 enzyme system on the enzyme concentration (C) in a wide range of concentrations from C=10^{-6} M to C=10^{-11} M in the process of lauric acid (LA) substrate hydroxylation. A wider concentration range (as compared to the one studied earlier in [2]) has been studied for the following reasons.

(1) The concentration range below 10^{-9} M corresponds to the conditions of reduced enzymatic activity of CYP102A1. A shift of the equilibrium of the enzyme dimerization towards the formation of monomers with lower activity can be observed within this range [10].

(2) The enzyme concentration greater than 10^{-8} M corresponds to the concentration level of proteins in a cell.

Within the framework of the present study, a dependence of microwave radiation from the CYP102A1 enzyme system on the enzyme concentration in the solution has been studied in the process of catalytic cycle of the enzyme by monitoring the brightness temperature with a microwave radiometer sensor.

It has been demonstrated that the functioning of CYP102A1 enzyme system is accompanied by a microwave radiation within the frequency range from 3.4 to 4.2 GHz at enzyme concentrations from C=10^{-10} M to C=10^{-6} M. Moreover, the radiation has appeared to be concentration-dependent. In this way, at high enzyme concentration (~10^{-6} M), the radiation from the ES had the form of single sync pulses correlated to the time of stirring, i.e., mechanical excitation of the system. At lower enzyme concentration, the radiation had the form of pulse trains. At the enzyme concentration of 10^{-11} M, no radiation has been registered.

2. Materials and Methods

2.1. Reagents. Dulbecco modified phosphate buffered saline (10 mM, pH 7.2) containing 100 mM NaCl (PBS-D) was purchased from Pierce (USA). Deionized ultrapure water was obtained with a Simplicity UV system (Millipore, France). Lauric acid (sodium salt) and NADPH were purchased from Sigma (USA).

2.2. Proteins. Cytochrome CYP102A1 was kindly provided by Prof. S.A. Usanov, and it was expressed according to [11]. Sample solutions with CYP102A1 concentration from 10^{-6} M to 10^{-10} M were prepared based on a stock solution (50 μM in 25 mM potassium phosphate buffer) by serial tenfold dilution in a working PBS-D solution.

2.3. Catalytic Reaction in CYP102A1 System. A catalytic reaction in a reconstituted enzyme system was carried out in a measuring cell containing cytochrome CYP102A1 and its substrate – lauric acid (0.5 mM) in PBS-D (pH 7.2), according to the procedure similar to the one described in [12].

Briefly, the reaction was carried out by performing a two-step procedure as follows: (1) a reconstituted cytochrome CYP102A1 system was prepared and placed into the measuring cell; (2) the reaction was initiated by adding a NADPH aqueous solution (0.2 mM) into this cell. The measurement conditions were as follows: sample solution volume V = 200 μl, temperature $T_{solution}$=~23°C. The control values of brightness temperature (T_{br}) were measured for solutions of two types: (1) without NADPH as an electron donor and (2) without the protein.

2.4. Analytical Measurements. The protein concentration was measured by spectrophotometry. CYP102A1 absorption spectra were measured with an Agilent Model 8453 spectrophotometer (USA) at 25°C. The concentration of purified CYP102A1 was determined by the difference in absorption of carboxyl complex in its reduced form, with the use of extinction coefficient of 91 $mM^{-1}cm^{-1}$ to take into account an absorption difference at wavelengths of 450 nm and 490 nm in accordance with the technique described by T. Omura et al. [13].

An RTM-01 RES broadband radiometer with the operating range from 3.4 to 4.2 GHz was used as a microwave radiation detector. During the measurements of the brightness temperature of the solution, a buggy-whip antenna of the detector was entirely immersed into the sample solution, similar to [2]. As noted in Introduction, the radiometer measures the object's brightness temperature. The radiation power P in a frequency range of the radiometer operation Δf can be estimated as

$$P = kT_{br}\Delta f \quad (1)$$

where k is the Boltzmann constant, T is the brightness temperature, and Δf is the frequency bandwidth [14]. From

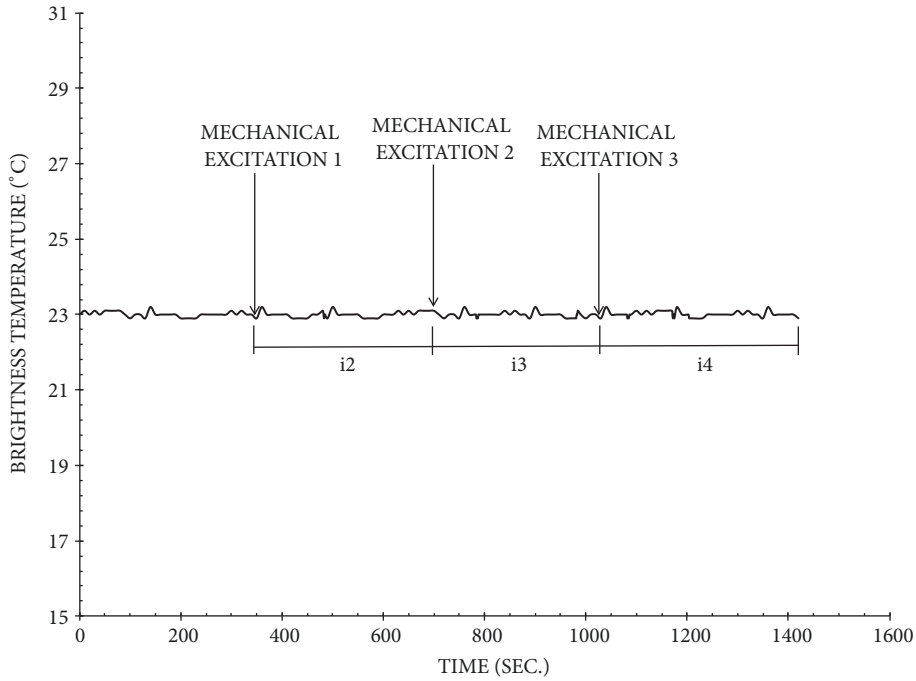

FIGURE 1: Example of effect of mechanical excitation on $T_{br}(t)$ dependence. Experiment conditions: inactive reconstituted CYP102A1 system, incubation mixture in a cell contained $C_{CYP102A1} = 10^{-6}$ M, 0.5 mM LA, 10 mM phosphate buffered saline (PBS-D), pH = 7.2, $V = 200\,\mu$l, $T_{solution}$=23°C. Arrows indicate the time of the solution stirring in a cell.

(1) one can see that the radiation power is directly proportional to the brightness temperature. Accordingly, shortly, for convenience, we estimate the radiation power (the energy of radiation in the frequency range Δf, further referred to as radiation energy) in centigrade degrees (°C). Accordingly, the data obtained are represented in the units of T_{br}, in which the RTM-01 RES radiometer is calibrated [2]. The measurement accuracy was ±0.1°C. The measurement results are presented in the form of T_{br} as a function of time t. Increase in T_{br} measured with the radiometer in the measuring cell during the catalytic reaction time t corresponds to the increase in the level of microwave radiation. During the catalytic reaction (after the addition of NADPH), the solution was stirred three times consecutively (mechanical excitation 1 (M. E. 1), mechanical excitation 2 (M. E. 2), mechanical excitation 3 (M. E. 3)). Accordingly, the range of measurements was, for convenience, divided into four subranges (i=4). As was previously demonstrated in [2], the generation of the microwave radiation from cytochrome CYP102A1 system occurs in the form of single pulses. For this reason, for each i subrange, we measured the range of changes in the amplitude of the pulses (in other words, the range of energy of the radiation in the pulses) of the generated microwave radiation. That is, ΔT^i_{br} is the pulse amplitude in i subrange, and the number of pulses (N_i) in this i subrange was counted. This allowed us to obtain the value of brightness temperature $T^i_{br} = (\Sigma N_i * T^i_{br})/N_i$ averaged over the number of pulses in this subrange. The energy of radiation for the measured frequency range in i subrange was calculated as $N_i * T^i_{br}$, and the total energy of radiation in the entire frequency range was calculated as the sum of the energy of radiation in all i subranges as $\Sigma N_i * T^i_{br}$.

3. Results

3.1. Results of Control Microwave-Radiation Measurements. The solution (1) containing both the enzyme and LA, but without NADPH, represents an inactive reconstituted cytochrome CYP102A1-containing enzyme system. To determine a baseline level of microwave-radiation noises in the inactive CYP102A1 enzyme system, the solution containing the enzyme (C=10^{-6}M) and LA, but without NADPH as an electron donor (Figure 1), was analyzed. To determine nonspecific effect of NADPH addition to the buffer solution on the level of microwave radiation, an enzyme-free solution (Figure 2) containing LA was used. NADPH was added to the solution, which was mechanically stirred three times (Figure 2).

Results of the control measurements have indicated that the brightness temperature T_{br} slightly increases both when the solution was mechanically stirred and when the components were nonspecifically added thereto. Hereafter, such an increase delimited noise signal of microwave radiation, which amounted to ±0.7°C. Figures 1 and 2 display representative results of the control measurements, where a noise pulse can be seen after NADPH is added or when the solution is stirred.

3.2. Microwave Radiation from CYP102A1 Solution at Various Enzyme Concentrations. The conditions for registration of a

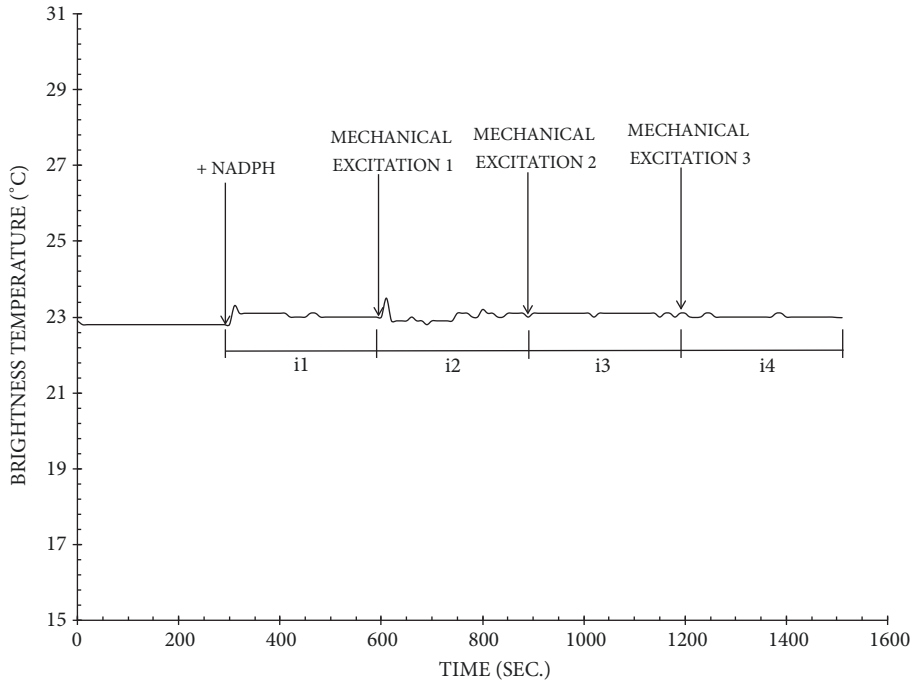

Figure 2: Example of effect of NADPH addition to a buffer on $T_{br}(t)$ dependence. Experiment conditions: incubation mixture in a cell contained 0.5 mM LA, 10 mM phosphate buffer saline (PBS-D), pH = 7.2, V = 200 μl, $T_{solution}$=23°C. Arrows indicate the time of addition of 0.2 mM NADPH as an electron donor to the system and that of the solution stirring in a cell.

microwave radiation from the enzyme solution during the catalytic cycle are described in Materials and methods.

Brightness temperature, T_{br}, of the solution was measured for the reconstituted cytochrome CYP102A1 system containing the enzyme (at concentration within 10^{-11} M to 10^{-6} M) and LA, with NADPH added thereto. A variation in the brightness temperature, T_{br}, of the sample solution during the enzyme reaction was registered at the protein concentration of 10^{-6} M, 10^{-7} M, 10^{-8} M, 10^{-9} M, and 10^{-10} M. No change in the brightness temperature, T_{br}, was registered for the system with the protein concentration of 10^{-11} M.

The parameters of the radiation from the enzyme system CYP102A1 within the concentration range from 10^{-11} M to 10^{-6} M are listed in Table 1.

An example of the obtained results for the time dependence of brightness temperature $T_{br}(t)$ after NADPH addition to the solution containing CYP102A1 (at C=10^{-10}M) and LA, is shown in Figure 3. From Figure 3, it is evident that $T_{br}(t)$ dependence graph features a pulse train; these pulses in the $T_{br}(t)$ dependence indicate that the protein solution generates a microwave radiation. Besides, these pulses may appear not immediately after the addition of NADPH, but rather with a delay, which is about 250 s in this case. As it will be demonstrated, at other concentrations, pulse trains may appear again or not appear at all after consecutive stirring. As can be seen in Figure 3, some short-term (pulse) variation in ΔT_{br}^{i} with amplitude from 0.9 to 1.7°C and duration of about 20 to 40 s could be observed within the entire observation period (1.500 s). The pulses in *i1* subrange included four separate peaks (1-4) with the duration from 20 to 40 s and peak 5 consisting from two subsequent peaks merged (5a and 5b) into a wider one with the duration of ~40 s. Amplitude of these five peaks (1-4, 5a and 5b) within the subrange was ΔT_{br}^{i} = 1.2 to 1.3°C, whereas the averaged value of ΔT_{br}^{i} was equal to 1.2°C over the entire *i1* subrange. In *i1* subrange, the maximum energy, released in the form of a single pulse, was equal to 1.3°C. Total energy release in *i1* subrange was ~7.2°C. For *i2, i3, i4* subranges, the total energy release amounted to ~ 5.2°C, ~0°C, and ~0°C, respectively. The accumulated energy released throughout the entire period of microwave-radiation measurement amounted to 11.4°C (Table 1). The total number of pulses within the full range was equal to 10 throughout the observation time of 1.500 s.

When the enzyme concentration was increased to 10^{-9} M (Figure 4, curve 1), pulse trains also appeared on a $T_{br}(t)$ dependence graph after the addition of NADPH to the system. Moreover, the number of pulses was equal to about 8 throughout the entire period of observation, whereas average pulse amplitude was virtually the same as in the case with 10^{-10} M enzyme concentration. The pulse duration remained similar as well. The pulse trains after initiation of enzyme reaction by adding NADPH appeared with a large delay and were observed after M. E. 2 at the 40^{th} s (Figure 4). The total energy release of radiation was equal to approx. 14.4°C throughout the entire observation period. It is well known that CYP102A1 enzyme exhibits high activity in dimeric state and that it consistently transits to this state, generally, at concentration of 10^{-9}M and higher [10]. Therefore, the experiments were repeated within the framework of our study, starting with the concentration above and further at

Table 1: Parameters of radiation generated in the reconstituted CYP102A1 enzyme system.

C, M	Sub-range (i)	τ, s	ΔT^i_{br} (T^i_{br})	N_i	$N_i * T^i_{br}$	$\Sigma N_i * T^i_{br}$	T^{av}_{br}	Type of radiation
10^{-10} (Figure 3)	1	250 (after NAPH)	1.2-1.3 (1.2)	6	7.2	11.4	11.4	Pulse train
	2	5 (after M. E. 1)	0.9-1.7 (1.3)	4	5.2			
	3			0				
	4			0				
10^{-9} (Figure 4 curve 1)	1			0		14.4	12.5±1.9	Pulse train
	2							
	3	40 (after M. E. 2)	1.2-3.6 (1.8)	5	9.0			
	4	50 (after M. E. 3)	0.9-3.2 (1.8)	3	5.4			
10^{-9} (Figure 4, curve 2)	1					10.5		Pulse train
	2							
	3							
	4	250 (after M. E. 3)	0.9-3.4 (2.1)	5	10.5			
10^{-8} (Figure 5, curve 1)	1			0		2.8	5.6±2.8	Single pulse + pulse train
	2	140 (after M. E. 1)	1.6	1	1.6			
	3	10 (after M. E. 2)	1.2	1	1.2			
	4			0				
10^{-8} (Figure 5, curve 2)	1					8.4		Single pulse + pulse train
	2	100 (after M. E. 1)	1.2-2.2 (1.8)	4	7.2			
	3	150 (after M. E. 2)	1.2	1	1.2			
	4							
10^{-7} (Figure 6, curve 1)	1					10.8	10.9±0.1	Single pulse + pulse train
	2							
	3	140 (after M. E. 2)	3.0	1	3.0			
	4	150 (after M. E. 3)	2.6-5.2 (3.9)	2	7.8			
10^{-7} (Figure 6, curve 2)	1			0		11.0		Single pulse
	2	200 (after M. E. 1)	6.2	1	6.2			
	3							
	4	220 (after M. E.3)	4.8	1	4.8			
10^{-6}(Figure 1, curve 1)	1			0		10.5	9.3±1.2	Single pulse (synchronized with M. E.)
	2	120 (after M. E. 1)	3.9	1	3.9			
	3	160 (after M. E. 2)	3.2	1	3.2			
	4	180 (after M. E. 3)	3.4	1	3.4			
10^{-6} (Figure 7 curve 2)	1			0		8.1		Single pulse (synchronized with M. E)
	2	120 (after M. E. 1)	3.3	1	3.6			
	3	160 (after M. E. 2)	2.4	1	2.4			
	4	180 (after M. E. 3)	2.4	1	2.4			

τ is the time delay of pulse generation after the addition of NADPH or stirring (M. E.); ΔT^i_{br} is the pulse amplitude in i sub-range; T^i_{br} is the average pulse amplitude in i sub-range; N_i is the number of pulses in i sub-range; $N_i * T^i_{br}$ is the energy of radiation in i sub-range; $\Sigma N_i * T^i_{br}$ is the total energy of radiation throughout the entire period of observation; T^{av}_{br} is the total energy of radiation, averaged over two experimental values.

higher values, in order to evaluate the consistent generation of radiation during the enzyme reaction. Figure 4 displays the results of two microwave-radiation experiments for the protein solution with 10^{-9}M concentration. From Figure 4, it is evident that when the experiment was repeated, a microwave radiation was generated in the form of a train of five large pulses with a considerable delay (after M. E. 3) (Figure 4, curve 2). Total energy release of radiation throughout the entire period of observation amounted to approximately 10.5°C, which exceeds the noise level, meaning a 1.5-fold scatter of total radiation energy for two experiment technical replicates. The averaged value of energy released in the form of radiation for two technical replicates was equal to about 12.5±1.9°C.

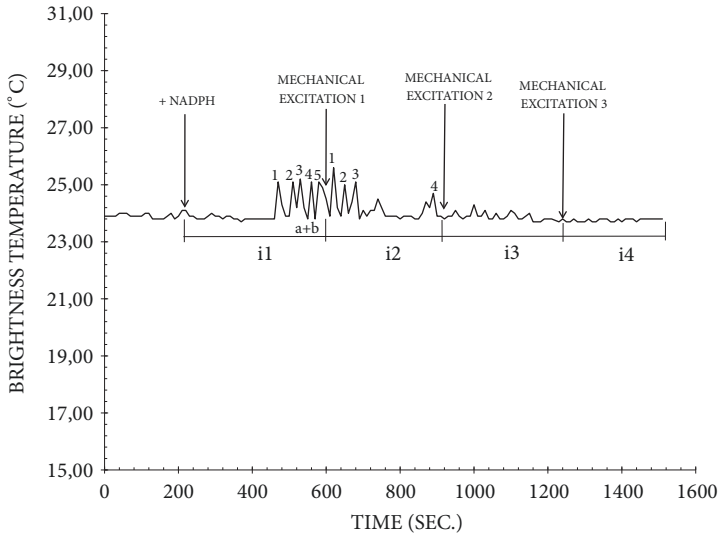

FIGURE 3: Example of $T_{br}(t)$ dependence in the reconstituted CYP102A1 system. Experiment conditions: $C_{CYP102A1} = 10^{-10}$ M, 10 mM phosphate buffered saline (PBS-D), pH = 7.2, $V = 200\ \mu$l, $T_{solution}$=23°C. Arrows indicate the time of addition of 0.2 mM NADPH as an electron donor to the system and that of the solution stirring in a cell.

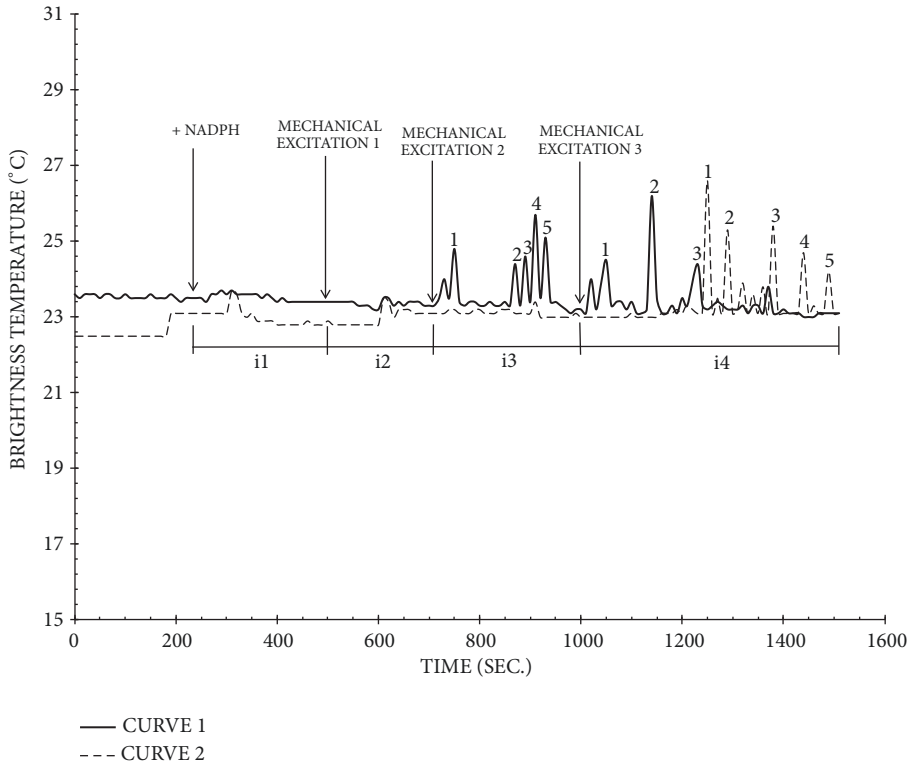

FIGURE 4: Example of $T_{br}(t)$ dependence in the reconstituted CYP102A1 system. Experiment conditions: $C_{CYP102A1} = 10^{-9}$ M, 10 mM phosphate buffered saline (PBS-D), pH = 7.2, $V = 200\ \mu$l, $T_{solution}$= 23°C. Arrows indicate the time of addition of 0.2 mM NADPH as an electron donor to the system and that of the solution stirring in a cell. Different line profiles indicate technical replicate 1 (curve 1, solid line) and technical replicate 2 (curve 2, dotted line).

When the enzyme concentration was increased to 10^{-8} M, two technical replicates were also conducted. Maximum number of pulses was observed in technical replicate 1 (see curve 2 in Figure 5). The number of pulses for this curve 2 was equal to four in the 1^{st} train, starting from the 100^{th} s after M. E. 1, and to one in the i3 subrange train at the 150^{th} s after M. E. 2 – technical replicate 2 (Figure 5, curve 2). Figure 5 displays typical results of the repeated experiment –

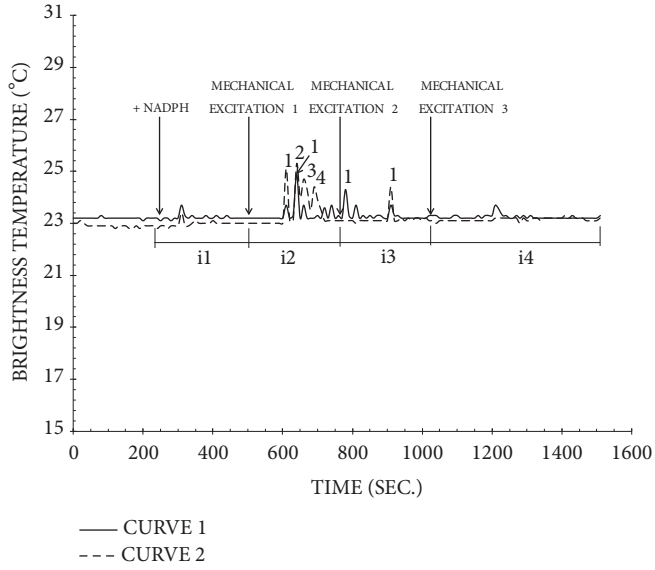

FIGURE 5: Example of $T_{br}(t)$ dependence in the reconstituted CYP102A1 system. Experiment conditions: $C_{CYP102A1} = 10^{-8}$ M, 10 mM phosphate buffered saline (PBS-D), pH = 7.2, V = 200 μl, $T_{solution}$=23°C. Arrows indicate the time of addition of 0.2 mM NADPH as an electron donor to the system and that of the solution stirring in a cell. Different line profiles indicate technical replicate 1 (curve 1, solid line) and technical replicate 2 (curve 2, dotted line).

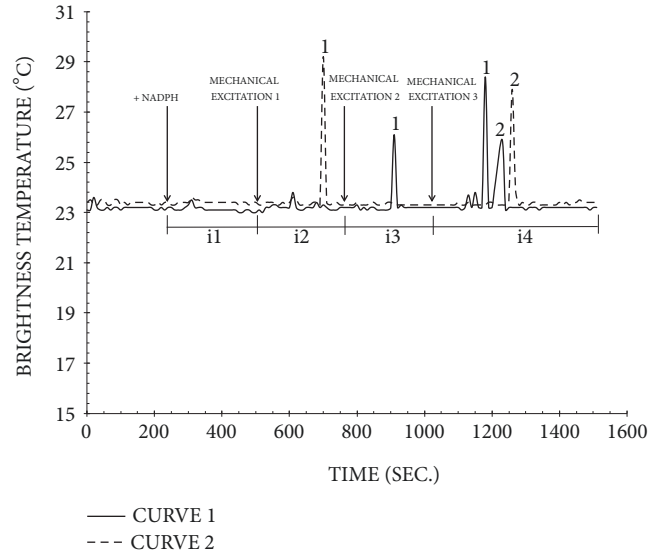

FIGURE 6: Example of $T_{br}(t)$ dependence in the reconstituted CYP102A1 system. Experiment conditions: $C_{CYP102A1} = 10^{-7}$ M, 10 mM phosphate buffered saline (PBS-D), pH = 7.2, V = 200 μl, $T_{solution}$=23°C. Arrows indicate the time of addition of 0.2 mM NADPH as an electron donor to the system and that of the solution stirring in a cell. Different line profiles indicate technical replicate 1 (curve 1, solid line) and technical replicate 2 (curve 2, dotted line).

technical replicate 1. It is clearly seen that the results obtained for radiation generated in the form of a pulse train are similar to those obtained for technical replicate 1 (the number of pulses was equal to one in the i1 subrange, starting from the 140^{th} s after M. E. 1, and to one in the i3 subrange at the 10^{th} s after M. E. 2.). The total energy released due to a microwave radiation amounted to 2.8°C and 8.4°C for the technical replicates 1 and 2, respectively. The total energy, released due to radiation and averaged over two technical replicates, was equal to 5.6±2.8°C. It should be noted that the pulse amplitude for curve 2 remained virtually the same as for C=10^{-9} M.

At 10^{-7} M enzyme concentration, a transition process featuring single pulses with high amplitude of ~5 to 6°C (Figure 6) could be observed. For curve 1, a single pulse appeared with a delay after M. E. 2 (after 140^{th} s), and two pulses appeared after M. E. 3 (150^{th} s). It is to be emphasized that the first pulse had very large amplitude (5.2°C). For curve

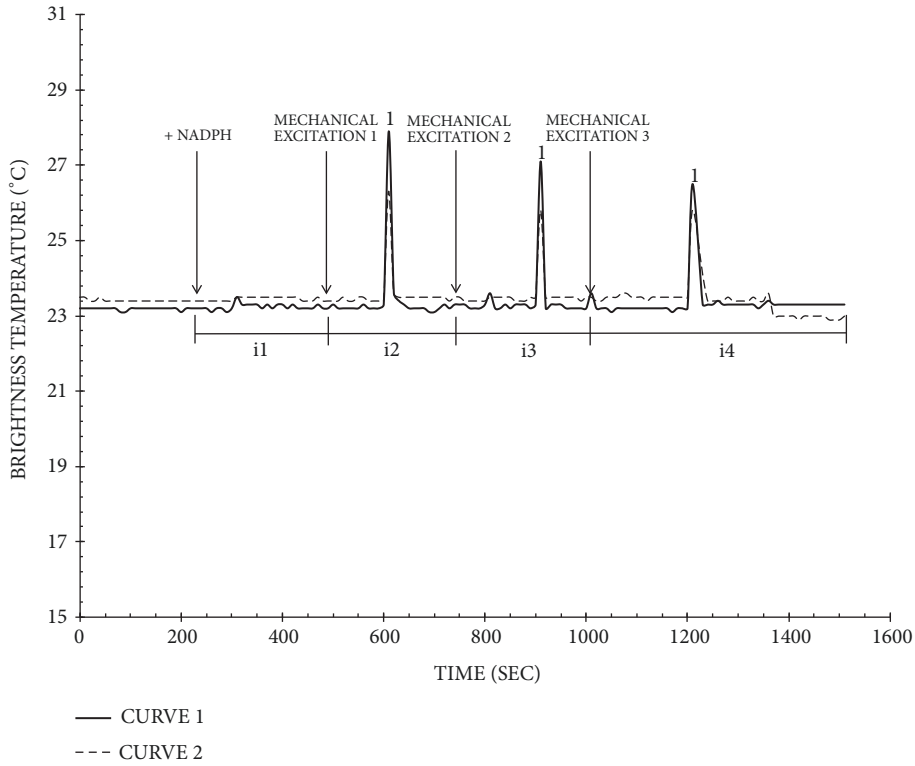

FIGURE 7: Example of $T_{br}(t)$ dependence in the reconstituted CYP102A1 system. Experiment conditions: $C_{CYP102A1} = 10^{-6}$ M, 10 mM phosphate buffered saline (PBS-D), pH = 7.2, V = 200 μl, $T_{solution}$=23°C. Arrows indicate the time of addition of 0.2 mM NADPH as an electron donor to the system and that of the solution stirring in a cell. Different line profiles indicate technical replicate 1 (curve 1, solid line) and technical replicate 2 (curve 2, dotted line).

2, after M. E. 1, a single 6.2°C high-amplitude pulse with a time delay of 200 s and after M. E. 3 the second pulse with a time delay of 220 s were observed. The radiation energy averaged over two technical replicates amounted to 10.9±1°C.

When the enzyme concentration was increased to 10^{-6} M, single pulses were observed. It is to be pointed out that in this case the time of generation of microwave pulses was synchronized with that of the solution stirring, i.e., mechanical excitation of the system for two technical replicates. Therefore, three pulses appeared one after another following each consequential excitation. At the same time, the pulse amplitude for curve 1 reached the values from 3.4 to 3.9°C (Figure 7). The total energy released throughout the period of observation was equal to 10.5°C (Figure 7, curve 1). The time dependence of the generation of single pulses synchronized with stirring could be observed for technical replicate 2 as well (Figure 7, curve 2). The total energy, released throughout the period of observation, amounted to 8.1°C. The radiation energy averaged over two technical replicates amounted to 9.3±1.2°C.

4. Discussion

As was mentioned in Introduction, the enzymatic activity of CYP102A1 was well described previously and was shown to be accompanied by a cyclic transition of spin states of iron heme and by vibrations of the enzyme molecule [10, 15–18]. In [17], the enzymatic activity of CYP102A1 during LA hydroxylation was measured based on the characteristic rate of specific NADPH oxidation under conditions of steady-state kinetics at 25°C in 50 mM potassium phosphate buffer (pH 7.0). Therein, the initial rate of NADPH oxidation at the enzyme concentration of no less than 5 nM was relatively constant and equal to 50 s^{-1}. At lower concentration, when CYP102A1 dimers were supposed to dissociate into monomers, the initial rate of NADPH oxidation amounted to 10 s^{-1}. Previously, it was demonstrated that the CYP102A1 enzyme system is able to generate a microwave radiation at C=10^{-9} M [2].

Within the framework of our present study, it has been demonstrated that the reconstituted CYP102A1 enzyme system generated a microwave radiation in the form of a pulse train at lower enzyme concentration (C=10^{-10} M) up until the concentration value of 10^{-11} M, when the radiation decayed. Such a decay can be ascribed to the reduced activity of the system resulting from a lower number of more active enzyme dimers in the solution, and this confirms that the radiation effect is connected with the enzyme functioning. When concentration of the protein solution was increased to 10^{-7} M, the number of pulses in multiphoton radiation mode decreased with the increase in amplitude of an individual pulse. Subsequent increasing of the enzyme concentration

up to 10^{-6} M resulted in functioning of the enzyme system in a single-pulse mode with high pulse amplitude. Such a process can be explained based on an assumption that an aqueous-based protein medium features nonequilibrium domain structure. As is known, water is a heterogeneous medium with the spin nonequilibrium defined by the ratio between ortho- and para-isomers [19]. It is also known that enzyme additionally contributes to inhomogeneity due to generation of ice-type water clusters, shifting the equilibrium towards higher portion of ortho-isomers of water in the solution [20]. Astrophysical microwave masers based on rotational transitions of OH and ortho-H_2O were found in nature [20]. In [20], it was noted that rotational transitions of OH, H_2O, and H_2O_2 occur in the solution as well.

It is a known fact that functioning of cytochrome CYP102A1 leads to the development of active OH forms and hydrogen peroxide. These active OH forms can radiate within a microwave frequency range, so ortho-H_2O can radiate in this range. The radiation generated by active OH forms and by other active forms of molecules can initiate excitation of ortho-H_2O levels and transitions between ortho- and para-isomers of water. The transitions between ortho- and para-H_2O are possible owing to the following: (1) water represents a nonequilibrium mixture of two liquids, overheated (in terms of spin temperature) to 230°C [21]; (2) water is susceptible to super-weak disturbances in particular temperature points [22]; (3) water represents a mixture characterized by a trigger-like avalanche switching [19]. The pulse train appearing within a microwave band in the enzyme system in a second-long interval (which is much larger than the characteristic enzyme turnover time equal to 0.02 s [10]) can cause a combined radiation of active forms of molecules, stimulated by enzyme reaction in various areas (domains) of the aqueous-based enzyme medium. Previously, during experimental studies of this enzyme system by atomic force microscopy, it was found that catalytic activity of CYP102A1 manifested itself through fluctuations of the protein globule in a Herz frequency range [23]. The average time between them was about several seconds. Such low-frequency fluctuations coincided with the vibration frequency of large water clusters [24].

According to our data obtained for a wide range of the enzyme concentrations (from 10^{-10} M to 10^{-6} M), the energy released in the form of a microwave radiation falls approximately within the same range of values, considering high fluctuation of its average value. It means that microwave radiation is accompanied not only by generation, but also by decay; i.e., it is a complex process. This complex process of CYP102A1 enzyme system radiating is defined by several factors, among which we can distinguish the following: (1) viscosity inhibiting the transition between ortho and para states of water molecule under the conditions of spin nonequilibrium of water [20]; (2) radiation factor due to domain activity of the aqueous-based enzyme medium, related to the increase in the number of functioning enzymes. At low concentrations, domains radiate discretely, out of sync, on a pulse train basis. With increasing the enzyme concentration, (1) viscosity of the solution increases, thus inhibiting ortho-/para-transition, what leads to lower total radiation energy and (2) radiation factor increases as well due to a higher number of functioning enzymes. When the concentration reaches critical values (C=10^{-6} M), radiation from these enzymes self-synchronizes. This process is similar to electromagnetic radiation in conventional maser systems, in which the radiation is stimulated and synchronized in active maser environment by the radiation itself, with a feedback based on active forms of molecules. As can be supposed, a transition to the enzyme single-pulse mode is related to synchronized radiation of all aqueous-based enzyme domains, and manifests itself, possibly, as a biomaser-like effect. Once again, the fact of existence of ortho-H_2O maser should be emphasized [20, 25]. The processes involved in the generation of a microwave radiation can also include absorption of radiation by inactive OH forms, transition of water [24] structured in enzyme products of higher order than dimers, and other processes to be studied in the future.

Again, it should be noted that when the enzyme concentration is increased from 10^{-10} to 10^{-6} M, the microwave radiation energy generated per one pulse increases. At the same time, we can observe more pronounced interaction between CYP102A1 molecules in a structured aqueous medium transitioning cyclically in the process of catalysis, due to the lower distance between protein molecules (at C=10^{-6} M, the distance between molecules is about 100 nm). The enzyme concentration of 10^{-6} M is in agreement with the characteristic number of molecules per cell with the characteristic size of 1 μm. At such enzyme concentration, natural systems can transit from one state to another as well, which can form the basis for the functioning of the organism as a quantum computer.

Quantum computer is a computing device employing phenomena of quantum mechanics, such as quantum superposition and quantum entanglement, for data transmission and processing and for handling low-level information cells, specifically, qubits of values of 0 and 1 at the same time. Hypothetically, capabilities of a quantum computer allow for simultaneous processing of all possible states, achieving substantial superiority over conventional computers for a number of algorithms [26]. A quantum system of L two-level quantum elements (quantum bits, qubits) has 2^L linearly independent states. This means that state space of such quantum register is a 2^L-dimensional Hilbert space, according to quantum superposition principle. Any quantum computing operation corresponds to rotation of a register-state vector within the space. Therefore, a quantum computing device of L qubits actually uses simultaneously 2^L classical states. Any object that has two quantum states, such as polarization states of photons, electronic states of isolated atoms or ions, and spin states of atomic nuclei, can be considered as a physical qubit-implementing system. In our case, spin state of the aqueous-based enzyme domains with a specific ratio between ortho- and para-states of water therein, as well as with different spin states of iron heme of the enzyme, can serve as a qubit-implementing system. Qubit entanglement can occur in the aqueous-based enzyme system owing to the interaction of the aqueous-based enzyme domains,

correlation between which leads to a uniform quantum state. With the use of various mechanisms, including those with a radiation-based principle of operation, such interaction can be observed in living cells, as well as in an organism, featuring central nervous system, whose life-sustaining activity is also accompanied by other factors exciting spin transition of water, e.g., electric pulses generated during the functioning of blood circulatory and nervous system due to a triboelectric effect [27, 28]. It should be noted that the possibility of enhancement of the parameters of radiation from an enzyme system by means of its stimulation with electric pulses was demonstrated with the example of another heme-containing peroxidase system [29]. Therefore, spin states of aqueous domains of the protein and phases of their fluctuation can be employed for generation of qubits in a living system.

The concentration effect of transition of nonsynchronized radiation into the pulse-synchronized one in enzyme systems, as has been detected herein, can be employed in the future for mathematical modeling of the functioning of living systems, monitoring of living cell status, and development of novel noninvasive methods for diagnostics of diseases. Moreover, the effect registered herein can be employed in the development of next-generation quantum computers built with the use of biocomposite materials.

5. Conclusion

With the use of an RTM-sensor, it has been found that microwave radiation is generated during lauric acid (LA) hydroxylation by a heme-containing enzyme CYP102A1 within the enzyme concentration range from 10^{-10} M to 10^{-6} M. The type of radiation depends on the enzyme concentration. At low enzyme concentration (from 10^{-10} M to 10^{-8} M) such radiation has the form of pulse trains, while at high concentration (10^{-6} M) the radiation has the form of single pulses synchronized with external mechanical excitation of the enzyme system. It has been discussed that the discovered radiation effect can occur due to a biomaser-like generation. Such effect can be used to register activity of enzyme systems in a radio-frequency range. In the future, it can be a key to the development of novel systems for monitoring of functional state of living cell status, noninvasive methods for diagnostics of diseases, and next-generation quantum computers built with the use of biocomposite materials.

Data Availability

The data used to support the findings of this study are available from the corresponding author upon request.

Conflicts of Interest

The authors declare that they have no competing interests.

Acknowledgments

The work was performed in the framework of the Program for Basic Research of State Academies of Sciences for 2013-2020.

References

[1] R. S. Negrin and C. H. Contag, "In vivo imaging using bioluminescence: a tool for probing graft-versus-host disease," *Nature Reviews Immunology*, vol. 6, no. 6, pp. 484–490, 2006.

[2] Y. Ivanov, K. Malsagova, A. Izotov et al., "Detection of microwave radiation of cytochrome CYP102 A1 solution during the enzyme reaction," *Biochemistry and Biophysics Reports*, vol. 5, pp. 285–289, 2016.

[3] Y. D. Ivanov, K. A. Malsagova, T. O. Pleshakova, S. G. Vesnin, V. Y. Tatur, and K. N. Yarygin, "Monitoring of brightness temperature of suspension of follicular thyroid carcinoma cells in shf range by radiothermometry," *Pathological Physiology and Experimental Therapy*, vol. 60, no. 4, Article ID 29244941, pp. 174–177, 2016.

[4] S. V. Zinoviev and A. V. Ivanov, "Functional microwave thermography of primary malignant tumors: an experimental study," *Medical physics*, vol. 4, no. 76, pp. 51–58, 2017.

[5] L. O. Narhi and A. J. Fulco, "Characterization of a catalytically self-sufficient 119,000-dalton cytochrome P-450 monooxygenase induced by barbiturates in Bacillus megaterium," *The Journal of Biological Chemistry*, vol. 261, no. 16, Article ID 3086309, pp. 7160–7169, 1986.

[6] I. F. Sevrioukova, H. Li, H. Zhang, J. A. Peterson, and T. L. Poulos, "Structure of a cytochrome P450-redox partner electron-transfer complex," *Proceedings of the National Acadamy of Sciences of the United States of America*, vol. 96, no. 5, pp. 1863–1868, 1999.

[7] A. I. Archakov and G. I. Bachmanova, *Cytochrome P450 and Active Oxygen*, Taylor & Francis, New York, NY, USA, 1990.

[8] Y. Miura and A. J. Fulco, "(Omega -2) hydroxylation of fatty acids by a soluble system from bacillus megaterium," *The Journal of Biological Chemistry*, vol. 249, no. 6, pp. 1880–1888, 1974.

[9] S. Black and S. Martin, "Evidence for conformational dynamics and molecular aggregation in cytochrome P450 102 (BM-3)," *Biochemistry*, vol. 33, no. 40, pp. 12056–12062, 1994.

[10] R. Neeli, H. M. Girvan, A. Lawrence et al., "The dimeric form of flavocytochrome P450 BM3 is catalytically functional as a fatty acid hydroxylase," *FEBS Letters*, vol. 579, no. 25, pp. 5582–5588, 2005.

[11] A. B. Carmichael and L.-L. Wong, "Protein engineering of Bacillus megaterium CYP102: The oxidation of polycyclic aromatic hydrocarbons," *European Journal of Biochemistry*, vol. 268, no. 10, pp. 3117–3125, 2001.

[12] S. C. Maurer, H. Schulze, R. D. Schmid, and V. B. Urlacher, "Immobilisation of P450 BM-3 and an NADP+ cofactor recycling system: towards a technical application of heme-containing monooxygenases in fine chemical synthesis," *Advanced Synthesis & Catalysis*, vol. 345, pp. 802–810, 2003.

[13] T. Omura and R. Sato, "The carbon monoxide-binding pigment of liver microsomes. i. evidence for its hemoprotein nature," *The Journal of Biological Chemistry*, vol. 239, pp. 2370–2378, 1964.

[14] A. V. Vaysblat, *Radiotermography as Method of Medical Diagnostics*, 2003.

[15] H. M. Girvan, H. L. Toogood, R. E. Littleford et al., "Novel haem co-ordination varients of flavocytochrome P450 CYP102A1," *Biochemical Journal*, vol. 417, pp. 65–76, 2009.

[16] M. Noble, C. Miles, S. Chapman et al., "Roles of key active-site residues in flavocytochrome P450 BM3," *Biochemical Journal*, vol. 339, pp. 371–379, 1999.

[17] C. F. Oliver, S. Modi, W. U. Primrose, L. Y. Lian, and G. C. Roberts, "Engineering the substrate specificity of Bacillus megaterium cytochrome P-450 BM3: hydroxylation of alkyl trimethylammonium compounds," *Biochemical Journal*, vol. 327, pp. 537–544, 1997.

[18] S. S. Boddupalli, R. W. Estabrook, and J. A. Peterson, "Fatty acid monooxegention by cytochrome P-450 CYP102A1," *The Journal of Biological Chemistry*, vol. 265, no. 8, pp. 4233–4239, 1990.

[19] S. M. Pershin, "Conversion of ortho-para H2O isomers in water and a jump in erythrocyte fluidity through a microcapillary at a temperature of 36.6±0.3∘C," *Physics of Wave Phenomena*, vol. 17, no. 4, pp. 241–250, 2009.

[20] S. Pershin, "Signal exchange between bio-objects on the basis of carrier modulation: coherent radiation of astrophysical OH (1.6 to 1.7 GHz) and H_2O (22.3 GHz) masers," in *Proceedings of Workshop School "Volna 2011"*, pp. 54–57, 2011.

[21] S. M. Pershin and A. F. Bunkin, "Temperature evolution of the relative concentration of the H_2O ortho/para spin isomers in water studied by four-photon laser spectroscopy," *Laser Physics*, vol. 19, no. 7, pp. 1410–1414, 2009.

[22] S. V. Stebnovskii, "On the shear strength of structured water," *Technical Physics. The Russian Journal of Applied Physics*, vol. 49, no. 1, pp. 19–21, 2004.

[23] Y. D. Ivanov, N. S. Bukharina, T. O. Pleshakova et al., "Atomic force microscopy visualization and measurement of the activity and physicochemical properties of single monomeric and oligomeric enzymes," *Biophysics*, vol. 56, no. 5, pp. 892–896, 2011.

[24] A. V. Syroeshkin, A. N. Smirnov, V. V. Goncharuk et al., "Water as a heterogeneous structure," *Electronic Journal "It is investigated in Russia"*, pp. 843–854, 2006.

[25] V. S. Streľnitskiĭ, "Cosmic masers," *Soviet Physics Uspekhi*, vol. 17, no. 4, pp. 507–527, 1975.

[26] A. Ersov, "Quantum supremacy," *Popular Mechanics*, vol. 5, pp. 54–59, 2018.

[27] Y. D. Ivanov, A. F. Kozlov, R. A. Galiullin et al., "Influence of a pulsed electric field on charge generation in a flowing protein solution," *Separations*, vol. 5, no. 2, p. 29, 2018.

[28] Y. D. Ivanov, A. F. Kozlov, R. A. Galiullin, V. Y. Tatur, N. D. Ivanova, and V. S. Ziborov, "Influence of chip materials on charge generation in flowing solution in nanobiosensors," *Applied Sciences*, vol. 9, no. 4, p. 671, 2019.

[29] Y. D. Ivanov, A. F. Kozlov, K. A. Malsagova et al., "Monitoring of microwave emission of HRP system during the enzyme functioning," *Biochemistry and Biophysics Reports*, vol. 7, pp. 20–25, 2016.